Published in final edited form as:
Cell Metab. 2009 September ; 10(3): 167–177. doi:10.1016/j.cmet.2009.08.001.

TGR5-mediated bile acid sensing controls glucose homeostasis

Charles Thomas[1,7], **Antimo Gioiello**[2], **Lilia Noriega**[1,3,8], **Axelle Strehle**[1,8], **Julien Oury**[1,8], **Giovanni Rizzo**[4], **Antonio Macchiarulo**[2], **Hiroyasu Yamamoto**[1,3], **Chikage Mataki**[1,3], **Mark Pruzanski**[4], **Roberto Pellicciari**[2], **Johan Auwerx**[1,3,5,6], and **Kristina Schoonjans**[1,3,6]

[1]Institut de Génétique et Biologie Moléculaire et Cellulaire, CNRS / INSERM / ULP, 67404 Illkirch, France [2]Dipartimento di Chimica e Tecnologia del Farmaco, Università di Perugia, 06123 Perugia, Italy [3]Laboratory of Integrative and Systems Physiology, Ecole Polytechnique Fédérale de Lausanne, 1015 Lausanne, Switzerland [4]Intercept Pharmaceuticals, New York, NY 10013, USA [5]Institut Clinique de la Souris, 67404 Illkirch, France

Summary

TGR5 is a G-protein coupled receptor expressed in brown adipose tissue and muscle where its activation by bile acids triggers an increase in energy expenditure and attenuates diet-induced obesity. Using a combination of pharmacological and genetic gain- and loss-of function studies *in vivo*, we show here that TGR5 signaling induces intestinal glucagon-like peptide-1 (GLP-1) release, leading to improved liver and pancreatic function and enhanced glucose tolerance in obese mice. In addition, we show that the induction of GLP-1 release in enteroendocrine cells by 6α-ethyl-23(*S*)-methyl-cholic acid (EMCA, INT-777), a specific TGR5 agonist, is linked to an increase of the intracellular ATP/ADP ratio and a subsequent rise in intracellular calcium mobilization. Altogether, these data show that the TGR5 signaling pathway is critical in regulating intestinal GLP-1 secretion *in vivo* and suggest that pharmacological targeting of TGR5 may constitute a promising incretin-based strategy for the treatment of diabesity and associated metabolic disorders.

Keywords

Bile acids; G-protein-coupled receptor; GPR131; TGR5; glucagon-like peptide 1; energy homeostasis; insulin sensitivity; diabesity; Type 2 Diabetes; metabolic disorders

Introduction

Bile acids (BAs) have evolved over the past few years from being considered as simple lipid solubilizers to complex metabolic integrators (Houten et al., 2006; Thomas et al., 2008; Zhang

6Correspondence: Johan AUWERX or Kristina SCHOONJANS: Laboratory of Integrative and Systems Physiology (LISP), Ecole Polytechnique Fédérale de Lausanne, Station 15, 1015 Lausanne, Switzerland. Phone: +41 21 693 95 22, Fax: +41 21 693 96 00, admin.auwerx@epfl.ch.
[7]Current address: Center of PhenoGenomics, Ecole Polytechnique Fédérale de Lausanne, 1015 Lausanne, Switzerland
[8]These authors contributed equally to this work.

Disclosure

JA and RP consult for and GR and MP are employed by Intercept Pharmaceuticals, a company that develops therapeutics targeting bile acid receptors.

and Edwards, 2008). Beyond the orchestration of BA, lipid and glucose metabolism by the nuclear receptor farnesoid X receptor (FXR), BAs also act as signaling molecules through the BA-dedicated G-protein coupled receptor (GPCR) TGR5 (GPR131) (Kawamata et al., 2003; Maruyama et al., 2002). Stimulation of the TGR5 signaling pathway confers to BAs the ability to modulate energy expenditure by controlling the activity of type 2 deiodinase and the subsequent activation of thyroid hormone in brown adipose tissue (BAT) and muscle. In accordance with this, pharmacological intervention with a diet containing 0.5% of cholic acid (CA) efficiently attenuates diet-induced obesity (DIO) in mice (Watanabe et al., 2006). These results have indicated that TGR5 could be a promising target for the treatment of metabolic disorders associated with weight gain. In addition, expression of TGR5 has recently been described in enteroendocrine L-cells (Reimann et al., 2008) and enteroendocrine cell lines, such as the STC-1 cells (Katsuma et al., 2005), which secrete the incretin, glucagon-like peptide-1 (GLP-1), upon nutrient intake. The therapeutic relevance of GLP-1 is currently well established since enhancement of the half-life of GLP-1 upon treatment with dipeptidyl peptidase 4 inhibitors (DPP4i) or activation of the GLP-1 receptor by exendin-4 derivatives (Ex-4) have been proven efficacious in the treatment of type 2 diabetes (Drucker, 2006; Drucker and Nauck, 2006). Therefore, the direct stimulation of intestinal GLP-1 release could constitute another promising GLP-1-based therapeutic approach for the treatment of metabolic diseases.

In this context, we hypothesized that TGR5 could play a critical *in vivo* role in the control of intestinal GLP-1 release and in the maintenance of glucose homeostasis. This assumption was investigated *in vivo* using a combination of gain- and loss-of function genetic approaches. Additionally, we identified and explored the therapeutic properties of semi-synthetic cholic acid (CA) derivative, 6α-ethyl-23(*S*)-methyl-cholic acid (EMCA, INT-777), a potent TGR5 agonist with no FXR activity, which could hold promise for the treatment of diabesity.

Results

TGR5 activation stimulates GLP-1 release from enteroendocrine L-cells by enhancing mitochondrial oxidative phosphorylation and calcium influx

We report here a semi-synthetic cholic acid (CA) derivative, 6α-ethyl-23(*S*)-methyl-CA (EMCA, INT-777) as a selective and potent TGR5 agonist (Figure 1A and B). The rational for selecting this compound was based on previous *in vivo* work showing that CA induces energy expenditure via activation of TGR5 (Watanabe et al., 2006) and on structure-activity studies showing that alkyl substitutions at positions 6α and 23(*S*) improve the potency and selectivity of chenodeoxycholic acid (CDCA) towards TGR5 (Pellicciari et al., 2007; Sato et al., 2008). The addition of these alkyl substitutions to CA improved the resulting compound's EC_{50} on TGR5 by 30 fold (Figure 1B), while critically reducing its activity on FXR (Figure S1A). In accordance with previous studies, activation of TGR5 (Katsuma et al., 2005; Kawamata et al., 2003; Maruyama et al., 2002) by INT-777 triggered a dose-dependent increase in intracellular cAMP levels in enteroendocrine STC-1 cells (Figure 1C). This induction was abrogated upon reduction of TGR5 expression by a specific TGR5 shRNA (Figure 1C), illustrating the specificity of the compound. The specificity of INT-777 for TGR5 was further confirmed by its inability to activate a subset of nuclear receptors involved in lipid and xenobiotic metabolism (Figure S1A), as well as other GPCRs that are phylogenetically related to TGR5 (Figure S1B and C).

Since we previously established a link between BAs and energy expenditure *in vivo* (Watanabe et al., 2006), we have speculated that activation of TGR5 signaling could impact mitochondrial activity in a more general fashion. To find initial support for this hypothesis, we analyzed TGR5 mRNA expression *via* the GeneNetwork liver mRNA database in the BxD genetic reference population (www.genenetwork.org). A wide range of variation in TGR5 mRNA expression was evident among the different BxD mouse strains (Figure S2A). Interestingly, TGR5 mRNA

expression was highly significantly correlated with the expression of several genes encoding for subunits of complexes involved in oxidative phosphorylation, such as cytochrome c oxidase (Cox) (*e.g* CoxVI1a; Figure 1D) and ATP synthase (Atp6v0b, ATPase H+ transporting V0 subunit B; Atpaf2, ATP synthase mitochondrial F1 complex assembly factor 2; Atp1a3, ATPase Na+/K+ transporting alpha 3 polypeptide; Atp6v1b2, ATPase H+ transporting V1 subunit B isoform 2; Figure S2B). Consistent with this observation, treatment of STC-1 cells with INT-777 resulted in a cAMP-dependent increase in Cox activity (Figure 1E), that was associated with an increase in cellular oxygen consumption (Figure 1F) and a raise in the ATP/ADP ratio (Figure 1G). This result was confirmed in the human enteroendocrine cell line NCI-H716 in which INT-777 treatment increased ATP production in a cAMP-dependent manner (figure S3A). Interestingly, TGR5 expression was also strongly correlated with that of Kir6.2, a component of the ATP-dependent potassium channel (K_{ATP}) (Figure 1H). These correlations were further corroborated by TGR5 RNA interference in STC-1 cells, which resulted in a concomitant drop in the expression of CoxIV and Kir6.2 mRNAs (Figure 1I).

In pancreatic beta cells, it is well established that an increase in the ATP/ADP ratio derived from glucose metabolism closes the K_{ATP} channels, resulting in depolarization of the plasma membrane. This membrane depolarization in turn opens calcium-gated voltage channels (Ca_v), causing calcium influx. The resultant increase in intracellular calcium then triggers the direct interaction between exocytotic proteins situated in the insulin-containing granule membrane and those located in the plasma membrane (Yang and Berggren, 2006), leading to the subsequent release of insulin (Nichols, 2006). Recent findings support the hypothesis that K_{ATP} and Ca_v channels also plays a pivotal role in GLP-1 release from enteroendocrine L cells (Reimann and Gribble, 2002; Reimann et al., 2008). Fascinatingly, in the BxD reference population we also found that TGR5 expression correlated with the expression of $Ca_v2.2$ (Figure 2A), whose expression was previously described in enteroendocrine cells (Reimann et al., 2005) and which participates in calcium-stimulated insulin release in pancreatic beta cells (Yang and Berggren, 2006). Along with this, INT-777 robustly increased calcium influx in the human enteroendocrine cell line NCI-H716, an effect that was potentiated by TGR5 over-expression and by contrast blunted by TGR5 RNA interference (Figure 2B and C) or by the addition of the adenylate cyclase inhibitor MDL-12330A (MDL) (Figure 2D). In addition, the presence of glucose enhanced the TGR5-dependent increase in intracellular calcium (Figure 2E). This effect was correlated with a rise in GLP-1 release from the NCI-H716 cells (Figure 2F), which was inhibited by MDL-12-330A (Figure S3B). The TGR5-mediated GLP-1 release triggered by INT-777 was further confirmed in the mouse enteroendocrine STC-1 cells in which the impact of INT-777 on GLP-1 release was enhanced by TGR5 over-expression, while being prevented either by RNA interference (Figure 2G) or by MDL-12-330A, further underscoring the cAMP-dependence of TGR5-mediated GLP-1 release (Figure 2H). Taken together, these data demonstrate that TGR5 regulates a key pathway governing the release of GLP-1 from enteroendocrine L-cells.

TGR5 overexpression modulates GLP-1 secretion in vivo

To further evaluate the metabolic role of enhanced TGR5 signaling, we assessed the impact of transgenic overexpression of TGR5 *in vivo* in the context of diet-induced obesity (DIO) in mice. TGR5 transgenic mice (TGR5-Tg) were generated by oocyte injection of the bacterial artificial chromosome (BAC) RP23-278N11 (Figure S4A). By quantitative real-time PCR, TGR5-Tg mice were shown to have integrated 6 copies of the RP23-278N11 BAC clone, leading to a robust TGR5 mRNA expression, restricted to most tissues that express TGR5 normally (Figure S4B). Glucose tolerance was markedly improved in TGR5-Tg mice challenged for 10 weeks with a high fat (HF) diet compared to control HF-fed littermates (Figure 3A), whereas no difference was noticed in mice on chow diet (CD) (data not shown). In contrast to our expectations, no differences were observed in body weight gain between

wild-type and TGR5-Tg mice on chow or high fat diet (Figure S5A and B), demonstrating that improvement of glucose tolerance in TGR5-Tg mice could not be attributed to the confounding effects of weight loss. The absence of weight gain in TGR5-Tg mice, in the wake of an increase in energy expenditure (Figure S5C) was explained by a reduction of locomotor activity (Figure S5D). Since, GLP-1 receptor knock-out mice display a marked hyperactivity (Hansotia et al., 2007), we administered the GLP-1 receptor agonist exendin-4 to wild-type mice in order to assess whether the decrease in locomotor activity in TGR5-Tg mice could be linked to GLP-1 secretion. Exendin-4 efficiently and dose-dependently reduced locomotor activity in mice. Interestingly, at 1nmol/Kg, we noticed a significant decrease in locomotor activity while the mice were still eating properly (Figure S5E and F).

Interestingly and according to our expectations, glucose tolerance in TGR5-Tg mice was associated with a robust GLP-1 secretion and insulin release in response to an oral glucose load (Figure 3B). The significance of the enhanced GLP-1 secretion was underscored by the fact that measurements of plasma GLP-1 levels were performed without preliminary oral administration of a dipeptidyl peptidase-4 (DPP4) inhibitor to the mice. This enhanced GLP-1 in TGR5-Tg helps to explain the decreased locomotor activity in TGR5-Tg mice. To further investigate the impact of TGR5 over-expression on GLP-1 secretion, the HF-fed mice were subsequently challenged with a test meal to stimulate BA release from the gallbladder. Interestingly, the impact of TGR5 overexpression on insulin and GLP-1 secretion was more pronounced postprandially than after simple glucose challenge (Figure 3C). We speculate that these effects are due to the increased BA flux triggered by the test meal as compared to the glucose challenge. In line with this hypothesis, the treatment of ileal explants from TGR5-Tg and control mice with lithocholic acid (LCA) confirmed that BAs provide an excellent signal to induce GLP-1 release in the context of high TGR5 expression (Figure 3D). These data are furthermore in accordance with results obtained in mTGR5-transfected STC-1 cells in which GLP-1 release was also boosted by increased expression of TGR5 (Figure 2G). We speculate that in the context of wild-type ileal explants the quick degradation of GLP-1 by dipeptidyl-peptidase 4 enzyme might mask the moderate increase in GLP-1 release triggered by LCA.

The impact of GLP-1 on pancreatic function has been extensively documented during the last decade and ranges from insulin-secretagogue effects to the promotion of pancreatic islet survival and proliferation (Drucker, 2006). In this context, immunofluorescent staining of insulin on pancreatic sections revealed that in contrast to hypertrophic islets with low insulin content, as observed in HF-fed control mice, islets of HF-fed TGR5-Tg mice were not hypertrophic and stained more intensively for insulin (Figure 3E). In line with these data, counting and sizing of pancreatic islets confirmed that TGR5 expression results in the maintenance of a normal islet distribution profile (Figure 3F), likely due to enhanced plasma GLP-1 levels. In addition, the insulin content of isolated pancreatic islets was significantly higher in HF-fed TGR5-Tg mice than in controls (Figure 3G).

To further establish a role of TGR5 signaling in the maintenance of glucose homeostasis, we assessed the glucose tolerance of germline TGR5 deficient mice ($TGR5^{-/-}$), generated by breeding mice in which the TGR5 allele was floxed with CMV-Cre transgenic mice (Figure S4C–F). In direct contrast with what was observed in TGR5-Tg mice, glucose tolerance was impaired in $TGR5^{-/-}$ mice challenged with a HF-diet for 8 weeks (Figure 3H), whereas no difference was observed in CD fed mice (data not shown). GLP-1 secretion was then tested by challenging $TGR5^{+/+}$ and $TGR5^{-/-}$ mice with an oral glucose load 30 minutes after the administration of saline or INT-777 alone or in combination with the DPP4 inhibitor (DPP4i), sitagliptin. Pre-administration of INT-777 moderately increased GLP-1 release after a glucose challenge in $TGR5^{+/+}$ mice (Figure 3I). This effect was, however, markedly more pronounced when DPP4i was co-administered as a consequence of its ability to prolong the half-life of plasma GLP-1 (Drucker and Nauck, 2006) (Figure 3I). In contrast, the effects of INT-777 on

plasma GLP-1 levels were blunted in TGR5$^{-/-}$ mice (Figure 3J). Together these data underscore the critical role of TGR5 signaling in the control of GLP-1 release and further demonstrate the specificity of the semi-synthetic agonist, INT-777, *in vivo*.

The TGR5 agonist INT-777 increases energy expenditure and reduces hepatic steatosis and obesity upon high fat feeding

In view of the improved glucose and insulin profile in TGR5-Tg mice, we next assessed the therapeutic potential of INT-777 admixed at a dose of 30 mg/kg/day (mkd) with the diet in an intervention study in C57BL/6J mice in which diabesity was induced by HF feeding for 14 weeks. As expected, the HPLC profile of plasma BAs confirmed the presence of INT-777 in the treated mice only (Figure 4A). The plasma levels of INT-777 were within the range of those of CA and β-muricholic acid (Figure S6A). It is noteworthy that INT-777 treatment affected neither plasma BA composition nor the expression profile of the enzymes involved in BA synthesis, whose expression is mainly under the control of nuclear receptors (Figure S6A–B). The complete absence of changes in the expression level of classical target genes of the farnesoid X receptor (FXR) in the liver, such as cholesterol 7α hydroxylase (CYP7A1) and bile salt export pump (BSEP) (Thomas et al., 2008), further confirmed the specificity of INT-777 towards TGR5 (Figure S6B).

After 10 weeks of treatment with INT-777, a significant attenuation of body weight gain of about 15%, in association with a sharp reduction in fat mass, was observed in HF-fed INT-777 treated mice relative to HF-fed controls (Figure 4B–C). The increase in liver and fat pad mass was also attenuated in HF-fed INT-777 treated mice (Figure 4D). As noticed in our previous study with CA (Watanabe et al., 2006), the decrease in brown adipose tissue (BAT) mass was related to a diminution of white adipose tissue (WAT) in the interscapular region (Figure 4D and data not shown). The metabolic changes between control HF-fed and INT-777-treated HF-fed mice were not caused by a reduced calorie intake (Figure 4E) or fecal energy loss (Figure S6C), but rather were the consequence of enhanced energy expenditure, as indicated by the measurement of O_2 consumption and CO_2 production during indirect calorimetry (Figure 4F). During the dark period, the respiratory quotient of INT-777-treated mice was significantly reduced, consistent with increased fat burning (Figure 4F). Gene expression profiling of BAT confirmed that activation of TGR5 signaling pathway triggers the increase of several mitochondrial genes involved in energy expenditure along with an induction of type 2 deiodinase gene expression (Figure 4G). The activation of the mitochondrial respiratory chain by INT-777 was further evidenced by measuring O_2 consumption in primary brown adipocytes isolated from C57BL/6J mice treated for 12h with INT-777. Addition of the uncoupling agent, carbonylcyanide-ptrifluoromethoxyphenylhydrazone (FCCP), boosted basal O_2 consumption in all conditions, but was significantly more pronounced in those treated with INT-777 (Figure 4H). In addition to the enhanced energy expenditure, liver function was also improved, as evidenced by the reduction in liver steatosis, which was assessed by oil-red-O staining (Figure 4I) and biochemical quantification of liver lipid content (Figure 4J). Moreover, plasma levels of liver enzymes were markedly reduced compared to HF-fed controls, correlating with the absence of liver fibrosis in liver sections of INT-777-treated mice stained with sirius red (Figure 4I and K). The improvement in liver function was also reflected by the significant drop in plasma triglycerides and non-esterified fatty acids (NEFA) in HF-fed mice treated with INT-777 (Figure 4L).

The TGR5 agonist INT-777 improves insulin sensitivity in obese mice

We also ascertained the ability of INT-777 to improve glucose homeostasis. In both DIO and db/db mice, an environmental and genetic model of diabesity, respectively, treatment with INT-777 (30 mkd) admixed with the diet robustly improved glucose tolerance after an oral challenge with glucose (Figure 5A and C), along with an improvement of the glucose-

stimulated insulin secretion profile (Figure 5B and D, lower panel). This feature is consistent with a GLP-1 mediated improvement in pancreatic function. Furthermore, fasting glucose and insulin levels were decreased in both DIO and db/db mice that were treated with INT-777 (Figure 5B and D, top panel). To further characterize the impact of INT-777 on glucose homeostasis and insulin sensitivity, a hyperinsulinemic euglycemic glucose clamp was performed on these DIO mice. Consistent with the improved glucose tolerance, the glucose infusion rate required to maintain euglycemia in DIO mice treated with INT-777 was virtually identical to that observed in CD-fed control mice (Figure 5E). While insulin-resistant HF-fed mice showed an increased endogenous production of hepatic glucose, together with a reduction of both glucose disposal rate and the suppression of glucose production by insulin, INT-777 treatment of HF-fed mice normalized these parameters to the values observed in CD-fed mice (Figure 5E). Measurement of insulin-stimulated ^{14}C-deoxy-glucose uptake during the hyperinsulinemic euglycemic glucose clamp indicated that the improvement in glucose homeostasis by INT-777 could be mainly attributed to reduced insulin-resistance in liver and muscle (Figure 5F). These effects correlated with normalization in the expression of key genes involved in hepatic glucose homeostasis (Figure 5G).

To address the specificity of INT-777 with regards to TGR5 in vivo, the impact of 4 weeks treatment with INT-777 at 30mkd on glucose tolerance was compared in TGR5$^{+/+}$ and TGR5$^{-/-}$ mice, primed by HF feeding for 9 weeks. Even over this short time period, INT-777 significantly improved glucose tolerance in TGR5$^{+/+}$ fed a HF diet (Figure 6A), along with a normalization of insulin secretion during oral glucose challenge (Figure 6B). These effects were blunted in TGR5$^{-/-}$ mice, thereby providing further arguments to support the specificity of INT-777 for TGR5 (Figure 6A and B).

Discussion

Following our previous demonstration that TGR5 activation governs energy metabolism in BAT and muscle (Watanabe et al., 2006) and inspired by the fact that TGR5 is expressed in enteroendocrine cells (Katsuma et al., 2005; Reimann et al., 2008), we explored in this study whether TGR5 activation could alter glucose homeostasis. Our data demonstrate that GLP-1-producing enteroendocrine cells are not only sensitive to nutrients present in the intestinal lumen, such as glucose and lipids (Edfalk et al., 2008; Hirasawa et al., 2005; Overton et al., 2006; Reimann et al., 2008), but also to BAs, which activate the TGR5 signaling pathway. Along with the lipid sensing GPCRs, GPR40, GPR119 and GPR120 (Edfalk et al., 2008; Hirasawa et al., 2005; Overton et al., 2006; Reimann et al., 2008), TGR5 represents a key pathway for the regulation of intestinal GLP-1 release. TGR5-mediated GLP-1 release in enteroendocrine L-cells involves the closure/opening of the K_{ATP}/Ca_v channels through a modulation of mitochondrial oxidative phosphorylation and the subsequent change in ATP/ADP ratio. Modulating this TGR5-driven pathway is of therapeutic potential given that incretin-based therapies have emerged as potent anti-diabetic strategies (Drucker, 2006; Drucker and Nauck, 2006).

In addition to our observations on GLP-1 release *in vitro*, we demonstrated through a gain and loss-of-function genetic approach, that the TGR5 pathway is a crucial determinant of glucose homeostasis *in vivo*. In fact, the activation of TGR5 by the selective and potent TGR5 agonist INT-777, may constitute a way to stimulate the release of incretins, such as GLP-1, translating into beneficial metabolic effects that could be of use in the treatment of diabesity and associated metabolic disorders. Although the receptor is expressed in many tissues (Kawamata et al., 2003; Maruyama et al., 2002), activation of TGR5 with the CA-derived, INT-777, is particularly attractive, given the increased exposure of enteroendocrine cells in the gut due to the extensive enterohepatic recirculation of INT-777 with other BAs in the bile pool (data not shown). In this manner the efficiency of intestinal BA re-absorption considerably increases the

effective dose to which enteroendocrine cells are exposed. Despite these "gut-centered" properties of BAs and their derivatives, we cannot exclude the possibility that some of the beneficial metabolic actions of INT-777 may be unrelated to its modulation of GLP-1 levels. It is interesting to note within this context, that other GPCRs expressed in enteroendocrine cells, such as GPR119 (Chu et al., 2007), are also expressed in pancreatic beta cells (Chu et al., 2007; Sakamoto et al., 2006; Soga et al., 2005). We can therefore at present not exclude that some TGR5-mediated effect on insulin release and glucose tolerance could involve direct pancreatic effects that are partially independent of GLP-1. Further investigations, using a beta cell specific TGR5 deficient mouse model are required to test this assumption.

It should also be noted that, given the systemic bioavailability of INT-777 as evidenced by the plasma concentrations achieved, direct activation of TGR5 in other tissues is also a significant factor in the compound's effects *in vivo*. Indeed, in line with our previous experience with natural BAs (Watanabe et al., 2006), INT-777 also increased energy expenditure and attenuated weight gain upon high fat feeding through TGR5-mediated effects in BAT and muscle. The more limited impact of INT-777 on energy expenditure relative to our previous study using natural BAs can be attributed to the substantially lower doses of INT-777 that were administered in this study. Since the TGR5 signaling pathway has also been shown to be active in macrophages, further investigation is also required to evaluate the potential ameliorative effect of INT-777 on inflammatory processes, which also contribute to the metabolic syndrome (Despres and Lemieux, 2006).

Our current work also underscores the complexity of the endocrine activities of BAs, including TGR5- and FXR-mediated actions, which all integrate to maintain glucose homeostasis. TGR5-mediated effects of BAs appear to center on the stimulation of GLP-1 release and the subsequent improvement in insulin-secretion and pancreatic function (Drucker, 2006; Drucker and Nauck, 2006). BAs, that escape the first-pass hepatic clearance and end up in the systemic circulation (Angelin et al., 1982), then fine tune energy expenditure through activation of TGR5 in BAT and muscle with a resulting attenuation of weight gain (Watanabe et al., 2004). By contrast, so far no significant weight loss has been reported in the context of FXR-activation in mice (Duran-Sandoval et al., 2005; Ma et al., 2006; Watanabe et al., 2006; Zhang et al., 2006). Instead, FXR-mediated actions of BAs appear mainly to affect liver metabolism by increasing glycogen production (Duran-Sandoval et al., 2005; Ma et al., 2006; Zhang et al., 2006) and decreasing lipogenesis and VLDL production (Watanabe et al., 2004), thereby reducing hepatic glucose and fatty acid output, which in turn contributes to improved insulin sensitivity (Duran-Sandoval et al., 2005; Ma et al., 2006; Zhang et al., 2006).

The link between BAs and glucose homeostasis may not only be relevant in mice but also in humans. In support of this hypothesis, a correlation between BA levels and insulin sensitivity has already been evidenced in humans (Shaham et al., 2008). Interestingly, plasma BA levels were also found to be significantly higher in subjects after bariatric surgery than in matched obese patients, suggesting that BAs may contribute to the metabolic improvements of weight loss surgery (Patti et al., 2009). The inverse relationship between total BA concentration and 2 hour post-meal glucose levels, as well as the positive correlation between BAs and peak GLP-1 in that study, further indicates that also in humans BAs may be key regulators of GLP-1 release and glucose homeostasis (Patti et al., 2009).

In conclusion, by employing a combination of pharmacological and genetic gain- and loss-of-function genetic approaches, our studies show that the activation of the TGR5 signaling pathway counteracts the metabolic dysfunction associated with diabesity. TGR5 activation results in a range of beneficial metabolic effects that include resistance to weight gain and hepatic steatosis, preservation of liver and pancreatic function, and the maintenance of glucose homeostasis and insulin sensitivity. These effects are due to enhanced mitochondrial function

in muscle, BAT and enteroendocrine cells, resulting in an increase in energy expenditure and incretin secretion (Figure 7). This leads us to conclude that TGR5 agonists could represent potential promising agents for the management of diabesity, along with associated disorders such as nonalcoholic steatohepatitis (NASH).

Experimental procedures

Chemicals and reagents

All biochemical reagents were purchased from Sigma-Aldrich unless indicated. The DPP4 inhibitor (DPP4i) sitagliptin was a kind gift from Dr C. Ullmer (Hoffmann-La Roche). INT-777 was synthesized as previously described (Macchiarulo et al., 2008; Pellicciari et al., 2007).

Cell culture—*In vitro* experiments were carried out in STC-1 or NCI-H716 cells treated with vehicle (DMSO) or INT-777. INT-777 was assessed for its agonistic activity on TGR5 as previously described (Macchiarulo et al., 2008; Pellicciari et al., 2007). cAMP production was performed as described (Sato et al., 2008; Watanabe et al., 2006). Cytochrome C oxidase activity was evaluated by following the oxidation of fully reduced cytochrome C (Sigma) at 550 nm (Feige et al., 2008b). ATP/ADP ratio and GLP-1 release was measured according to the manufacturer's instruction (Biovision and Millipore, respectively). Primary brown adipocytes were prepared as previously described (Watanabe et al., 2006) and ileal explants were prepared according to an established method (Cima et al., 2004).

Intracellular calcium quantification—NCI-H716 (40000 cells) were seeded in 96 well black plates coated with Matrigel (BD Bioscience). 72h after transfection, cells were washed twice in assay buffer (HBSS1x, 20 mM Hepes, pH7.4) and assayed for intracellular calcium with Fluo-4 AM according to the manufacturer's protocol (Invitrogen).

Biochemistry and histochemistry—Plasma parameters and hepatic and fecal lipid content were measured as described (Mataki et al., 2007). Hematoxylin/eosin (HE), sirius red and oil-red-O stainings were performed as described (Mark et al., 2007) and micrographs were taken on wide-field microscopes (Leica) with a CCD camera. For pancreatic sections, islets were sized and counted from 4 HE-stained alternated sections spaced of 150 μM using Image J software (5 animals/group). Immunofluorescent staining of insulin was performed as described (Fajas et al., 2004). Additionally, pancreatic islets were isolated by collagenase digestion of pancreas from HF-fed TGR5-Tg mice according to online available procedures (www.jove.com/index/Details.stp?ID=255). Insulin was extracted after O/N incubation at −20°C in acid ethanol and measured by ELISA on PBS-diluted samples according to the manufacturer's instructions (Mercodia). GLP-1 release was measured in vitro, ex vivo and in vivo as described in supplemental experimental procedures.

Oxygen consumption measurement

Cellular oxygen consumption was measured using a Seahorse bioscience XF24 analyzer with 10 biological replicates per condition (Feige et al., 2008b).

Animal experiments—Animals were housed and bred according to standardized procedures (Argmann and Auwerx, 2006b). Age-matched male mice were used for all experiments. Genetically engineered mouse models (GEMMs), i.e. TGR5-Tg and TGR5$^{-/-}$ mice were generated as described in the supplementary information. Diet-induced obesity (DIO) in the GEMMs or C57BL/6J mice (Charles River) was induced by feeding 8-week-old mice with a HF-diet (60%Cal/fat, D12492; Research Diets) for at least 8 weeks, as mentioned in the text and figure legends. In the dietary intervention experiments, INT-777 was mixed with diet (Feige et al., 2008a) at the dose sufficient to reach an *in vivo* dose of 30mg/kg/d. Mouse

phenotyping experiments were performed according to EMPRESS protocols (http://empress.har.mrc.ac.uk) and aimed to assess food and water intake, body composition (Argmann et al., 2006a), energy expenditure (Argmann et al., 2006a), glucose and lipid homeostasis (Argmann et al., 2006b; Heikkinen et al., 2007; Mataki et al., 2007), and plasma biochemistry (Argmann and Auwerx, 2006a). Tissues and blood were collected and processed for histopathology, blood chemistry and gene expression, according to standardized procedures (Argmann and Auwerx, 2006a; Feige et al., 2008b; Mark et al., 2007; Watanabe et al., 2006). Hyperinsulinemic euglycemic clamp studies were performed as described (Feige et al., 2008b), with minor modifications including a change in the initial insulin bolus (30mU/kg) and insulin infusion rate (10mU/min/kg). Plasma GLP-1 levels were measured by ELISA (Millipore) on blood collected by retro-orbital puncture. Experiments with db/db mice (Charles River) were performed in 14-week-old animals fed a CD without or with INT-777 (30mg/kg/d) for 6 weeks (Feige et al., 2008a).

Gene expression profiling

Gene expression profiling was performed by real-time quantitative PCR (Feige et al., 2008b; Watanabe et al., 2006). Primer sequences used have been previously published except those used for the Kir6.2 gene: R- 5' AGATGCTAAACTTGGGCTTG, F- 5' TAAAGTGCCCACACCACTC.

Statistics

Statistical analyses were performed using the unpaired Student *t*-test. Data are expressed as mean ± S.E.M. and P values smaller than 0.05 were considered statistically significant.

Supplementary Material

Refer to Web version on PubMed Central for supplementary material.

Acknowledgements

We thank E. Garo, T. Meyer, E. Pierrel for technical help and and H. Sato for cloning of the mTGR5 cDNA. Technical support and discussions related to the generation of GEMMs and mouse phenotyping from E. Bedu, M.C. Birling, M.F. Champy, L. El Fertak, H. Meziane, L. Pouilly, X. Warot of the Mouse Clinical Institute is acknowledged. We thank N. Dali-Youcef of the Hopitaux Universitaire de Strasbourg for BA measurement, and L. Adorini, F. De Franco and D. Passeri from Intercept Pharmaceuticals for the assessment of the activity of INT-777 on GPCRs and nuclear receptors as well as for calcium and ATP measurement. Work was supported by grants from CNRS, INSERM, FRM, ANR PHYSIO 2007 (BASE), EU (EUGENE2), Ligue contre le cancer, ARC, Ecole Polytechnique Fédérale de Lausanne, and NIH (DK067320 and DK59820). CT is supported by an ARC fellowship.

References

Angelin B, Bjorkhem I, Einarsson K, Ewerth S. Hepatic uptake of bile acids in man. Fasting and postprandial concentrations of individual bile acids in portal venous and systemic blood serum. J Clin Invest 1982;70:724–731. [PubMed: 7119112]

Argmann CA, Auwerx J. Collection of blood and plasma from the mouse. Curr Protoc Mol Biol Chapter 2006a;29Unit 29A 23

Argmann CA, Auwerx J. Minimizing variation due to genotype and environment. Curr Protoc Mol Biol Chapter 2006b;29Unit 29A 22

Argmann CA, Champy MF, Auwerx J. Evaluation of energy homeostasis. Curr Protoc Mol Biol Chapter 2006a;29Unit 29B 21

Argmann CA, Houten SM, Champy MF, Auwerx J. Lipid and bile acid analysis. Curr Protoc Mol Biol Chapter 2006b;29Unit 29B 22

Chu ZL, Jones RM, He H, Carroll C, Gutierrez V, Lucman A, Moloney M, Gao H, Mondala H, Bagnol D, Unett D, Liang Y, Demarest K, Semple G, Behan DP, Leonard J. A role for beta-cell-expressed G

protein-coupled receptor 119 in glycemic control by enhancing glucose-dependent insulin release. Endocrinology 2007;148:2601–2609. [PubMed: 17289847]

Cima I, Corazza N, Dick B, Fuhrer A, Herren S, Jakob S, Ayuni E, Mueller C, Brunner T. Intestinal epithelial cells synthesize glucocorticoids and regulate T cell activation. J Exp Med 2004;200:1635–1646. [PubMed: 15596520]

Despres JP, Lemieux I. Abdominal obesity and metabolic syndrome. Nature 2006;444:881–887. [PubMed: 17167477]

Drucker DJ. The biology of incretin hormones. Cell Metab 2006;3:153–165. [PubMed: 16517403]

Drucker DJ, Nauck MA. The incretin system: glucagon-like peptide-1 receptor agonists and dipeptidyl peptidase-4 inhibitors in type 2 diabetes. Lancet 2006;368:1696–1705. [PubMed: 17098089]

Duran-Sandoval D, Cariou B, Percevault F, Hennuyer N, Grefhorst A, van Dijk TH, Gonzalez FJ, Fruchart JC, Kuipers F, Staels B. The farnesoid X receptor modulates hepatic carbohydrate metabolism during the fasting-refeeding transition. J Biol Chem 2005;280:29971–29979. [PubMed: 15899888]

Edfalk S, Steneberg P, Edlund H. Gpr40 is expressed in enteroendocrine cells and mediates free fatty acid stimulation of incretin secretion. Diabetes 2008;57:2280–2287. [PubMed: 18519800]

Fajas L, Annicotte JS, Miard S, Sarruf D, Watanabe M, Auwerx J. Impaired pancreatic growth, beta cell mass, and beta cell function in E2F1 (−/−)mice. J Clin Invest 2004;113:1288–1295. [PubMed: 15124020]

Feige JN, Lagouge M, Auwerx J. Dietary manipulation of mouse metabolism. Curr Protoc Mol Biol Chapter 2008a;29Unit 29B 25

Feige JN, Lagouge M, Canto C, Strehle A, Houten SM, Milne JC, Lambert PD, Mataki C, Elliott PJ, Auwerx J. Specific SIRT1 activation mimics low energy levels and protects against diet-induced metabolic disorders by enhancing fat oxidation. Cell Metab 2008b;8:347–358. [PubMed: 19046567]

Hansotia T, Maida A, Flock G, Yamada Y, Tsukiyama K, Seino Y, Drucker DJ. Extrapancreatic incretin receptors modulate glucose homeostasis, body weight, and energy expenditure. J Clin Invest 2007;117:143–152. [PubMed: 17187081]

Heikkinen S, Argmann CA, Champy MF, Auwerx J. Evaluation of glucose homeostasis. Curr Protoc Mol Biol Chapter 2007;29Unit 29B 23

Hirasawa A, Tsumaya K, Awaji T, Katsuma S, Adachi T, Yamada M, Sugimoto Y, Miyazaki S, Tsujimoto G. Free fatty acids regulate gut incretin glucagon-like peptide-1 secretion through GPR120. Nat Med 2005;11:90–94. [PubMed: 15619630]

Houten SM, Watanabe M, Auwerx J. Endocrine functions of bile acids. Embo J 2006;25:1419–1425. [PubMed: 16541101]

Katsuma S, Hirasawa A, Tsujimoto G. Bile acids promote glucagon-like peptide-1 secretion through TGR5 in a murine enteroendocrine cell line STC-1. Biochem Biophys Res Commun 2005;329:386–390. [PubMed: 15721318]

Kawamata Y, Fujii R, Hosoya M, Harada M, Yoshida H, Miwa M, Fukusumi S, Habata Y, Itoh T, Shintani Y, Hinuma S, Fujisawa Y, Fujino M. A G protein-coupled receptor responsive to bile acids. J Biol Chem 2003;278:9435–9440. [PubMed: 12524422]

Ma K, Saha PK, Chan L, Moore DD. Farnesoid X receptor is essential for normal glucose homeostasis. J Clin Invest 2006;116:1102–1109. [PubMed: 16557297]

Macchiarulo A, Gioiello A, Thomas C, Massarotti A, Nuti R, Rosatelli E, Sabbatini P, Schoonjans K, Auwerx J, Pellicciari R. Molecular field analysis and 3D-quantitative structure-activity relationship study (MFA 3D-QSAR) unveil novel features of bile acid recognition at TGR5. J Chem Inf Model 2008;48:1792–1801. [PubMed: 18698841]

Mark M, Teletin M, Antal C, Wendling O, Auwerx J, Heikkinen S, Khetchoumian K, Argmann CA, Dgheem M. Histopathology in mouse metabolic investigations. Curr Protoc Mol Biol Chapter 2007;29Unit 29B 24

Maruyama T, Miyamoto Y, Nakamura T, Tamai Y, Okada H, Sugiyama E, Itadani H, Tanaka K. Identification of membrane-type receptor for bile acids (M-BAR). Biochem Biophys Res Commun 2002;298:714–719. [PubMed: 12419312]

Mataki C, Magnier BC, Houten SM, Annicotte JS, Argmann C, Thomas C, Overmars H, Kulik W, Metzger D, Auwerx J, Schoonjans K. Compromised intestinal lipid absorption in mice with a liver-

specific deficiency of liver receptor homolog 1. Mol Cell Biol 2007;27:8330–8339. [PubMed: 17908794]

Nichols CG. KATP channels as molecular sensors of cellular metabolism. Nature 2006;440:470–476. [PubMed: 16554807]

Overton HA, Babbs AJ, Doel SM, Fyfe MC, Gardner LS, Griffin G, Jackson HC, Procter MJ, Rasamison CM, Tang-Christensen M, Widdowson PS, Williams GM, Reynet C. Deorphanization of a G protein-coupled receptor for oleoylethanolamide and its use in the discovery of small-molecule hypophagic agents. Cell Metab 2006;3:167–175. [PubMed: 16517404]

Patti, ME.; Houten, SM.; Bianco, AC.; Bernier, R.; Larsen, PR.; Holst, JJ.; Badman, MK.; Maratos-Flier, E.; Mun, EC.; Pihlajamaki, J.; Auwerx, J.; Goldfine, AB. Serum Bile Acids Are Higher in Humans With Prior Gastric Bypass: Potential Contribution to Improved Glucose and Lipid Metabolism. Silver Spring: Obesity; 2009.

Pellicciari R, Sato H, Gioiello A, Costantino G, Macchiarulo A, Sadeghpour BM, Giorgi G, Schoonjans K, Auwerx J. Nongenomic Actions of Bile Acids. Synthesis and Preliminary Characterization of 23- and 6,23-Alkyl-Substituted Bile Acid Derivatives as Selective Modulators for the G-Protein Coupled Receptor TGR5. J Med Chem 2007;50:4265–4268. [PubMed: 17685603]

Reimann F, Gribble FM. Glucose-sensing in glucagon-like peptide-1-secreting cells. Diabetes 2002;51:2757–2763. [PubMed: 12196469]

Reimann F, Habib AM, Tolhurst G, Parker HE, Rogers GJ, Gribble FM. Glucose sensing in L cells: a primary cell study. Cell Metab 2008;8:532–539. [PubMed: 19041768]

Reimann F, Maziarz M, Flock G, Habib AM, Drucker DJ, Gribble FM. Characterization and functional role of voltage gated cation conductances in the glucagon-like peptide-1 secreting GLUTag cell line. J Physiol 2005;563:161–175. [PubMed: 15611035]

Sakamoto Y, Inoue H, Kawakami S, Miyawaki K, Miyamoto T, Mizuta K, Itakura M. Expression and distribution of Gpr119 in the pancreatic islets of mice and rats: predominant localization in pancreatic polypeptide-secreting PP-cells. Biochem Biophys Res Commun 2006;351:474–480. [PubMed: 17070774]

Sato H, Macchiarulo A, Thomas C, Gioiello A, Une M, Hofmann AF, Saladin R, Schoonjans K, Pellicciari R, Auwerx J. Novel potent and selective bile acid derivatives as TGR5 agonists: biological screening, structure-activity relationships, and molecular modeling studies. J Med Chem 2008;51:1831–1841. [PubMed: 18307294]

Shaham O, Wei R, Wang TJ, Ricciardi C, Lewis GD, Vasan RS, Carr SA, Thadhani R, Gerszten RE, Mootha VK. Metabolic profiling of the human response to a glucose challenge reveals distinct axes of insulin sensitivity. Mol Syst Biol 2008;4:214. [PubMed: 18682704]

Soga T, Ohishi T, Matsui T, Saito T, Matsumoto M, Takasaki J, Matsumoto S, Kamohara M, Hiyama H, Yoshida S, Momose K, Ueda Y, Matsushime H, Kobori M, Furuichi K. Lysophosphatidylcholine enhances glucose-dependent insulin secretion via an orphan G-protein-coupled receptor. Biochem Biophys Res Commun 2005;326:744–751. [PubMed: 15607732]

Thomas C, Pellicciari R, Pruzanski M, Auwerx J, Schoonjans K. Targeting bile-acid signalling for metabolic diseases. Nat Rev Drug Discov 2008;7:678–693. [PubMed: 18670431]

Watanabe M, Houten SM, Mataki C, Christoffolete MA, Kim BW, Sato H, Messaddeq N, Harney JW, Ezaki O, Kodama T, Schoonjans K, Bianco AC, Auwerx J. Bile acids induce energy expenditure by promoting intracellular thyroid hormone activation. Nature 2006;439:484–489. [PubMed: 16400329]

Watanabe M, Houten SM, Wang L, Moschetta A, Mangelsdorf DJ, Heyman RA, Moore DD, Auwerx J. Bile acids lower triglyceride levels via a pathway involving FXR, SHP, and SREBP-1c. J Clin Invest 2004;113:1408–1418. [PubMed: 15146238]

Yang SN, Berggren PO. The role of voltage-gated calcium channels in pancreatic beta-cell physiology and pathophysiology. Endocr Rev 2006;27:621–676. [PubMed: 16868246]

Zhang Y, Edwards PA. FXR signaling in metabolic disease. FEBS Lett 2008;582:10–18. [PubMed: 18023284]

Zhang Y, Lee FY, Barrera G, Lee H, Vales C, Gonzalez FJ, Willson TM, Edwards PA. Activation of the nuclear receptor FXR improves hyperglycemia and hyperlipidemia in diabetic mice. Proc Natl Acad Sci U S A 2006;103:1006–1011. [PubMed: 16410358]

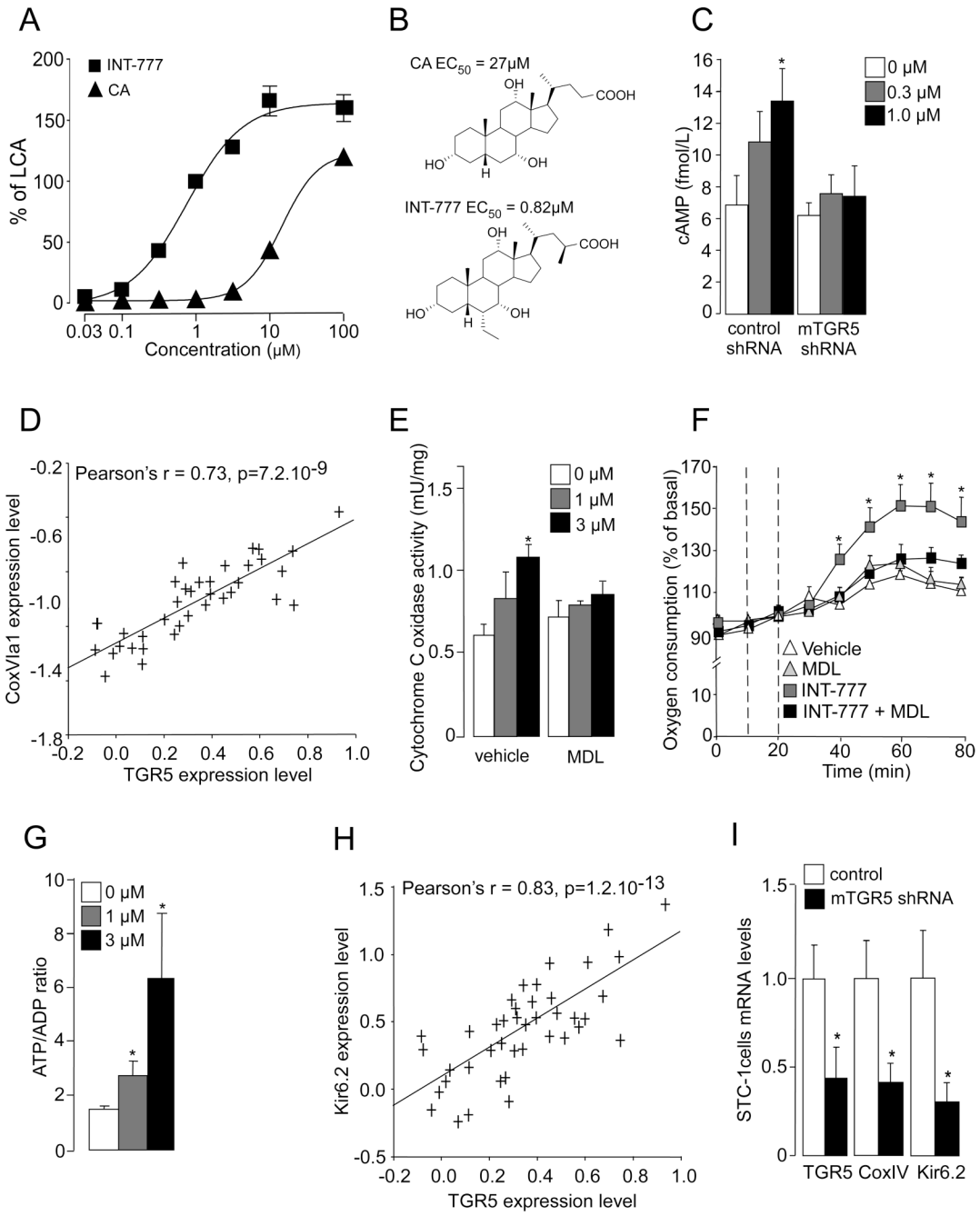

Figure 1. Activation of TGR5 signaling pathway activates mitochondrial oxidative phosphorylation and increases ATP/ADP ratio in enteroendocrine L cells

A. Activity of 6α-ethyl-23(*S*)-methyl cholic acid (INT-777) and cholic acid (CA) on TGR5 in CHO cells transiently transfected with human TGR5 expression vector and a Cre-Luc reporter vector. EC_{50} values are expressed as percent of the activity of 10 μM of LCA (n=3). **B**. Chemical structure of CA and INT-777 and respective TGR5 EC_{50}. **C.** Intracellular cAMP levels in STC-1 cells transfected with control or mTGR5 shRNA for 36 hr and treated with INT-777 at the concentrations indicated (n=3). **D**. Correlation plots for liver mRNA expression of TGR5 and CoxVI1a in the mouse BxD genetic reference population (n=41) as found in www.genenetwork.org and described in the supplemental methods. **E.** Cytochrome c oxidase

activity in STC-1 cells treated for 1hr with INT-777 at the concentration indicated. Vehicle or adenylate cyclase inhibitor MDL-12330-A (MDL) (1 μM) was added 15min prior to treatment (n=3). **F.** Oxygen consumption in STC-1 cells was measured using the XF24 extracellular flux analyzer (Seahorse Biosciences). The first vertical dotted line indicates the addition of vehicle or MDL-12330-A (MDL) to culture medium, the second dotted line depicts the treatment with INT-777 at 1 μM (n=10). **G**. ATP/ADP ratio in STC-1 cells treated as in panel (n=3). **H.** Correlation plots for liver mRNA expression of TGR5 and Kir6.2 in the mouse BxD genetic reference population according to a similar strategy as described in D. **I.** mRNA expression levels of TGR5, CoxIV, and Kir6.2 in STC-1 cells transfected for 36h with control or mTGR5 shRNA was measured by real-time quantitative PCR. Target mRNA levels were normalized to 36B4 mRNA levels (n=3). The data are represented as mean±SE. Student's unpaired *t*-test. * $P < 0.05$.

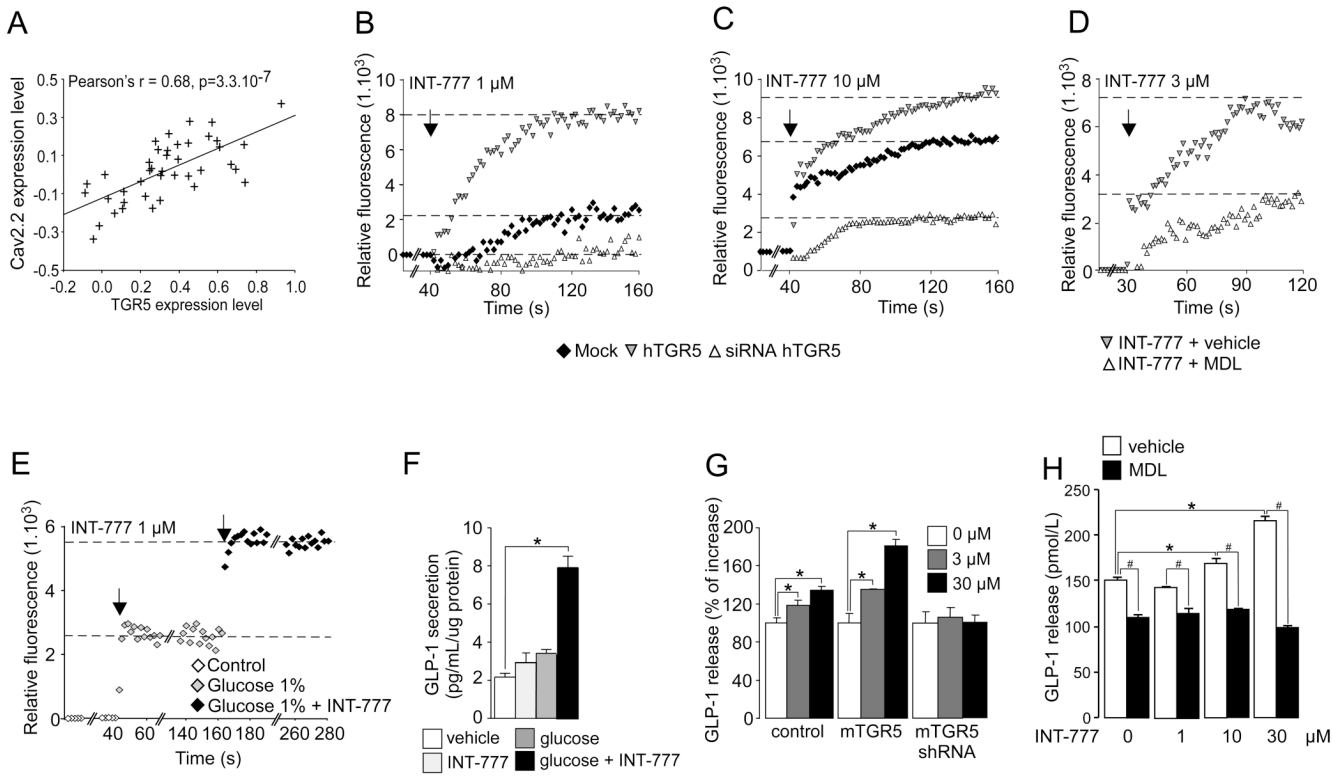

Figure 2. Activation of TGR5 signaling pathway increases intracellular calcium level and stimulates GLP-1 release in enteroendocrine L cells

A. Correlation plots for liver mRNA expression of TGR5 and Cav2.2 in the mouse BxD genetic reference population (n=41) as found in www.genenetwork.org and as described in the supplemental methods. **B–C**. Intracellular calcium level in NCI-H716 cells transfected with mock vector, hTGR5 expression vector or hTGR5 siRNA for 36 hr and treated with 1 µM (**B**) or 10 µM (**C**) of INT-777. The arrow represents INT-777 treatment (n=3). **D**. Intracellular calcium level in NCI-H716 cells treated with 3µM of INT-777 (indicated by the arrow) in the presence of vehicle or adenylate cyclase inhibitor MDL-12330-A (MDL) (10 µM). MDL or vehicle were added 15 min prior to INT-777 treatment (n=3). **E**. Intracellular calcium level in NCI-H716 cells treated with 1% glucose and then with 1 µM of INT-777 (n=3). **F.** GLP-1 release in NCI-H716 cells treated with 1% glucose or 1 µM of INT-777, or a combination of both agents (n=3). **G**: GLP-1 release in STC-1 cells transfected for 36h with control, mTGR5 expression vector or mTGR5 shRNA and then exposed 30 min to INT-777 at the indicated concentration. A DPP4 inhibitor (Millipore) was added into culture medium at 0.1% (n=3). **H.** Impact of 30 min of INT-777 treatment on GLP-1 release in STC-1 cells transfected with mTGR5 expression vector in the presence of vehicle or adenylate cyclase inhibitor MDL-12330-A (10 µM). MDL or vehicle were added 15 min prior to INT-777 treatment. A DPP4 inhibitor (Millipore) was added into culture medium at 0.1% (n=3). The data are represented as mean±SE. Student's unpaired *t*-test. * $P < 0.05$ vehicle vs INT-777 treatment, # $P < 0.05$ vehicle vs MDL-12330-A treatment.

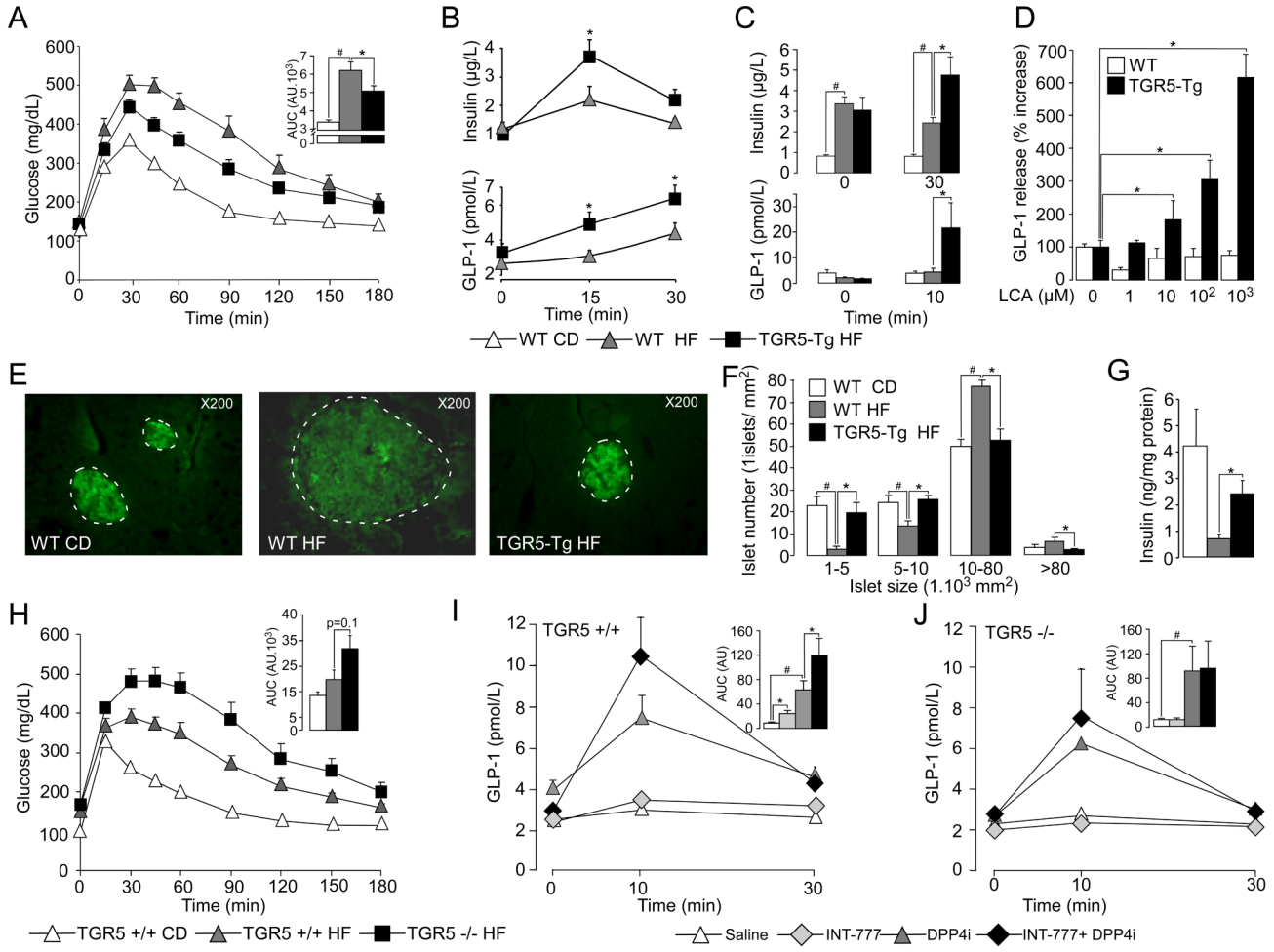

Figure 3. TGR5 signaling pathway modulates GLP-1 secretion *in vivo*

A. Oral glucose tolerance test (OGTT) in 10-weeks HF-fed TGR5-Tg male mice and CD/HF-fed age-matched male littermates. Body weight of TGR5-Tg and control littermates was 37.9 ±1.7g and 37.0±1.8g, respectively (n=8; not statistically different). The adjacent bar graph represents the average area under the curve (AUC) (n=8). **B–C.** Plasma levels of insulin (top panel) and GLP-1 (bottom panel) during OGTT (**B**) or before and after a test meal challenge (**C**) (n=8). **D.** GLP-1 release from ileal explants isolated from 18-weeks HF-fed control and TGR5-Tg male mice and exposed for 1hr to the indicated concentrations of LCA (n=4). **E.** Representative immunofluorescent insulin-stained pancreatic sections from CD and 20-weeks HF-fed control and TGR5-Tg male mice. **F.** Distribution profile of pancreatic islets from 20-weeks HF-fed control and TGR5-Tg male mice. Islets were counted and sized by the ImageJ analysis software on 4 hematoxylin eosin-stained alternated pancreatic sections spaced each by 150 µM (n=5). **G.** Insulin content in collagenase-isolated pancreatic islets from 20-weeks HF-fed control and TGR5-Tg male mice (n=5). **H.** OGTT in 8-weeks HF-fed $TGR5^{-/-}$ and $TGR5^{+/+}$ mice. The inset represents the average AUC. Body weight of $TGR5^{+/+}$ and $TGR5^{-/-}$ male mice at time of analysis was 46.3±3.9g and 51.9±2.0g, respectively (n=8; not statistically different). **I–J.** Plasma GLP-1 levels in CD-fed $TGR5^{+/+}$ (**I**) and $TGR5^{-/-}$ mice (**J**) after an oral glucose challenge preceded 30min before by the oral administration of saline or INT-777 (30 mg/kg), alone or in combination with a dipeptidyl-peptidase-4 inhibitor (DPP4i, 3mg/kg) (n=6). The data are represented as mean±SE. Student's unpaired *t*-test. *

($P < 0.05$) HF-fed compared to HF-fed INT-777-treated mice and # ($P < 0.05$) HF-fed *vs* CD-fed mice except for panels I and J where * assessed saline or DPP4i treated mice *vs* INT-777 or INT-777 + DPP4i treated mice and # saline *vs* DPP4i treated mice.

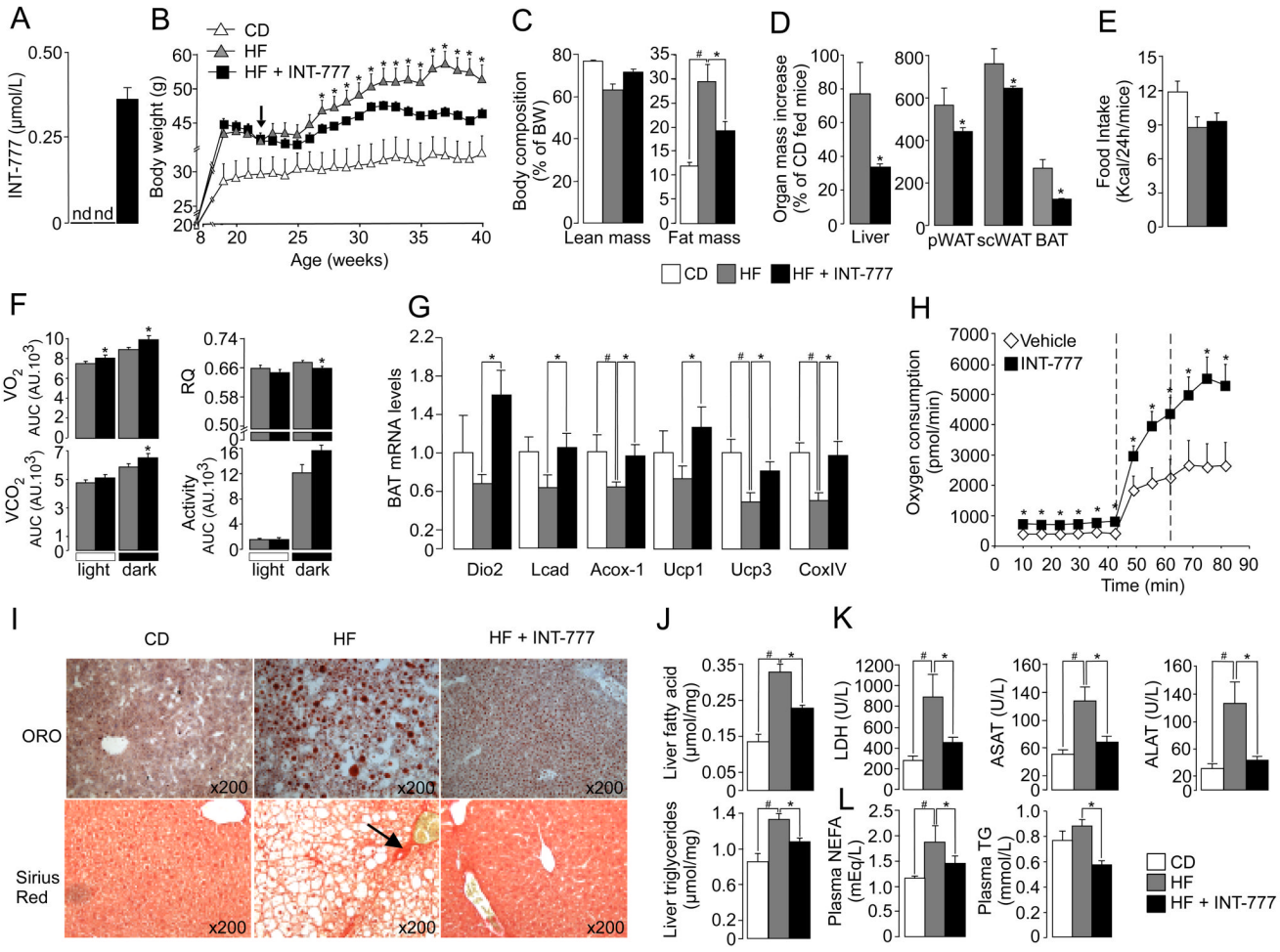

Figure 4. The TGR5 agonist INT-777 increases energy expenditure and reduces hepatic steatosis and adiposity in DIO mice

A. Measurement by HPLC of plasma INT-777 levels in CD-, HF- and HF-fed INT-777-treated male C57BL6/J mice. **B.** Dietary intervention with INT-777 (30mg/kg/d) was started after a 14-week period of HF feeding at the time indicated by the arrow. Body weight evolution in all groups was followed throughout the study (n=8). **C.** Body composition was assessed by qNMR after 8 weeks of dietary intervention (n=8). **D.** Organ mass was expressed as percent of the weight of CD-fed control mice. **E.** Food intake (n=8). **F.** Spontaneous horizontal activity and energy expenditure, evaluated by the measurement of oxygen consumption (VO_2) and carbon dioxide release (VCO_2) were monitored over a 18hr period 6 weeks after the initiation of the dietary intervention. The respiratory quotient (RQ) was calculated as the ratio VCO_2/VO_2. Bar graphs represent the average AUC. For the RQ, bar graphs represent the average (n=8). **G.** Gene expression in BAT by real-time quantitative PCR. Target mRNA levels were normalized to 36B4 mRNA levels (n=8). **H.** Primary brown adipocytes isolated from CD-fed C57BL/6J male mice were cultured for 12hr with vehicle or 3 µM of INT-777 and O_2 consumption was measured using the XF24 extracellular flux analyzer (Seahorse Biosciences) (n=5). The dotted lines illustrate the addition of the uncoupling agent FCCP at successive doses of 250 nM and 500 nM. **I.** Representative pictures of oil-red-O (ORO) staining of cryosections (top panel) and sirius red staining of paraffin-embedded sections (bottom panel) of the liver at the end of the dietary intervention. Fibrosis is indicated by the arrow **J.** Lipid content in liver samples extracted according to the Folch's method (n=8). **K–L.** Plasma levels of liver enzymes (**K**)

and lipids (**L**) at the end of the dietary intervention (n=8). The data are represented as the mean ± SE. Student's unpaired *t*-test. * ($P < 0.05$) HF-fed compared to HF-fed INT-777 treated mice and # ($P < 0.05$) HF-fed *vs* CD-fed mice.

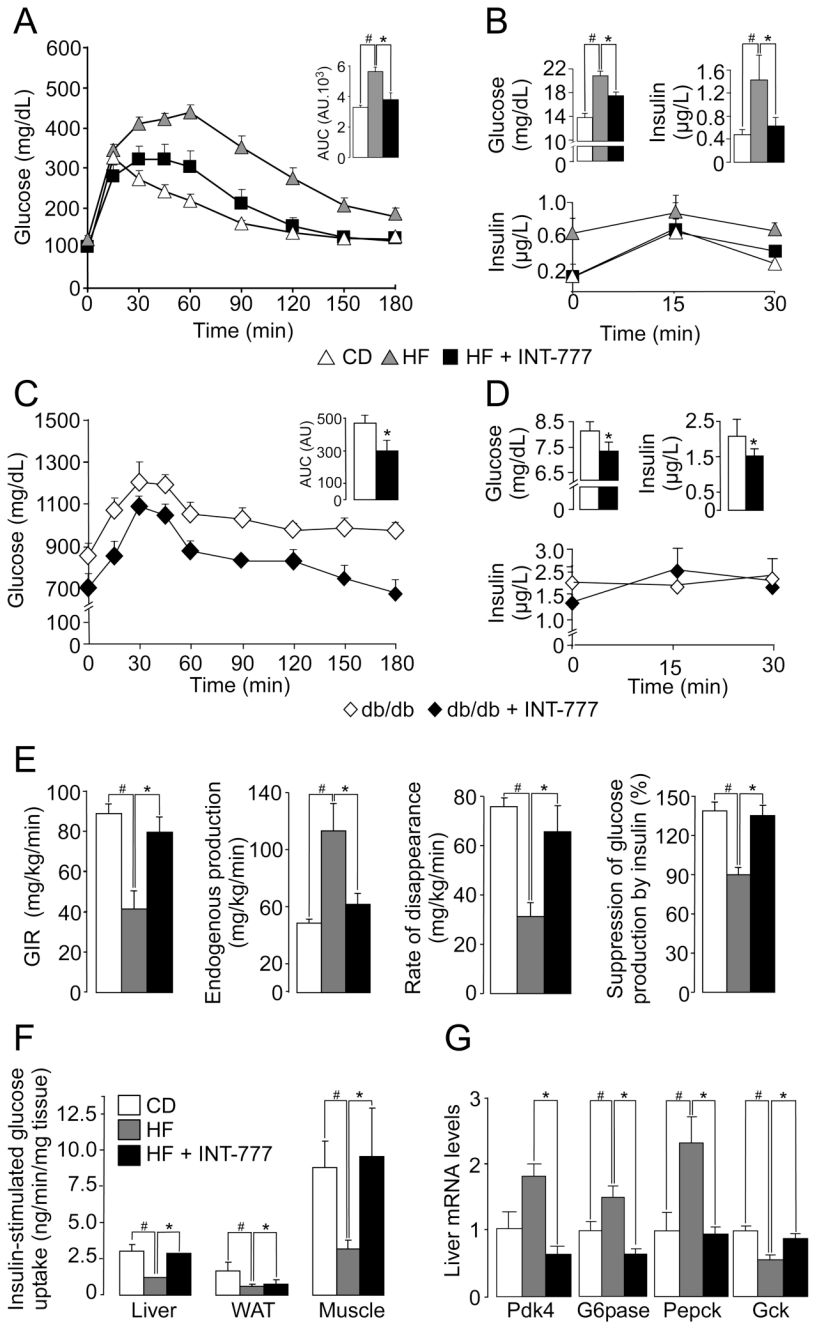

Figure 5. The TGR5 agonist INT-777 improves insulin sensitivity in obese mice

A. OGTT in CD- and HF-fed male C57BL6/J mice supplemented with 30mg/kg/d INT-777 for 8 weeks following the onset of obesity induced by feeding a HF diet during 10 weeks. The inset represents the average AUC. Body weight of vehicle and INT-777 treated mice was 38.08 ±1.83g and 32.26±0.95g, respectively (n=8; $P < 0.05$). **B.** Fasting glycemia and insulinemia (4h fasting) in DIO mice after 3 weeks of dietary intervention with INT-777 (top panel). Plasma insulin levels during OGTT in DIO mice (bottom panel). **C.** OGTT in 14-week-old CD-fed db/db male mice treated with 30mg/kg/d INT-777 for 6 weeks. The inset shows the average AUC (n=8). **D.** Fasting (4h) glycemia and insulinemia in db/db mice after 6 weeks of treatment with INT-777 (top panel). Plasma insulin levels during OGTT in DIO mice (bottom panel).

E. Insulin sensitivity evaluated through the average glucose infusion rate at equilibrium (euglycemia) in a hyperinsulinemic euglycemic clamp (10mU insulin/min/kg) in DIO mice (following the onset of obesity induced by feeding a HF diet during 10 weeks) after 10 weeks of dietary intervention with INT-777 (30mg/kg/d) (n=5). The evaluation of liver glucose production and its suppression by insulin, as well as the rate of glucose disappearance, was assessed at equilibrium using ^{3}H-glucose (n=5). **F.** Insulin-stimulated glucose uptake in the indicated tissues was measured using ^{14}C-2-deoxy-glucose tracers (n=5). **G.** Gene expression profiling in liver was performed by real-time quantitative PCR. Target mRNA levels were normalized to 36B4 levels (n=8). The data are represented as mean±SE. Student unpaired *t*-test. * ($P < 0.05$) HF-fed compared to HF-fed INT-777 treated mice and $^{\#}$ ($P < 0.05$) HF-fed *vs* CD-fed mice.

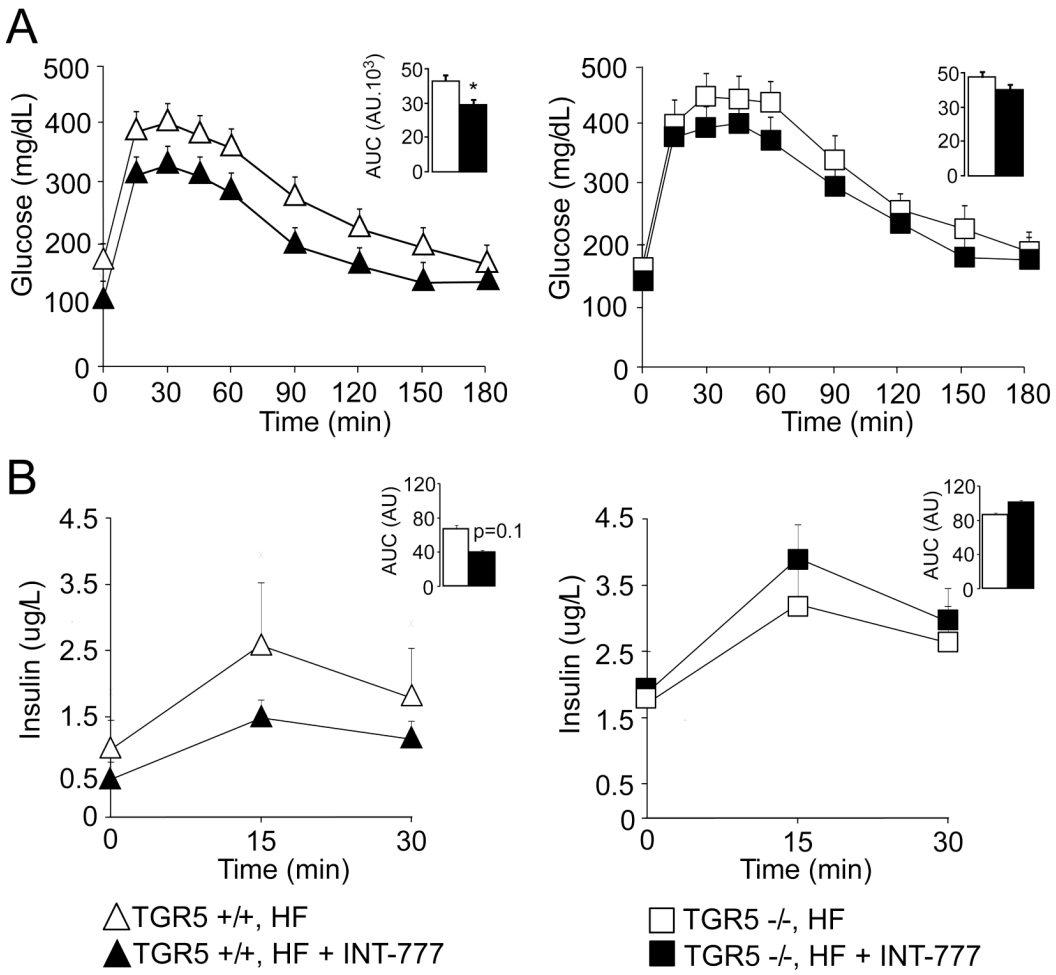

Figure 6. INT-777 mediated improvement of glucose tolerance is TGR5-dependent

A. $TGR5^{+/+}$ and $TGR5^{-/-}$ male mice were fed a HF diet for 9 weeks and a first OGTT was performed thereafter. HF was then supplemented with INT-777 at 30mg/kg/d. A second OGTT was performed 4 weeks after treatment with INT-777 was initiated. Curves represent glucose tolerance before and after 4 weeks treatment with INT-777 in $TGR5^{+/+}$ (left panel) and $TGR5^{-/-}$ (right panel) mice. The inset represents the average AUC. In $TGR5^{+/+}$ mice, body weight before and after INT-777 treatment was 46.86±3.54g and 43.50±3.47g, respectively (n=8; not statistically different). In $TGR5^{-/-}$ mice, body weight before and after INT-777 treatment was 54.34±2.23g and 52.30±2.72g, respectively (n=8; not statistically different). **B.** Plasma insulin levels were concurrently measured during the OGTT in DIO in $TGR5^{+/+}$ (left panel) and $TGR5^{-/-}$ (right panel) mice before and after 4 weeks treatment with INT-777. The inset represents the average AUC (n=8). The data are represented as mean±SE. Student's unpaired *t*-test. * ($P < 0.05$) Vehicle compared to INT-777 treated mice

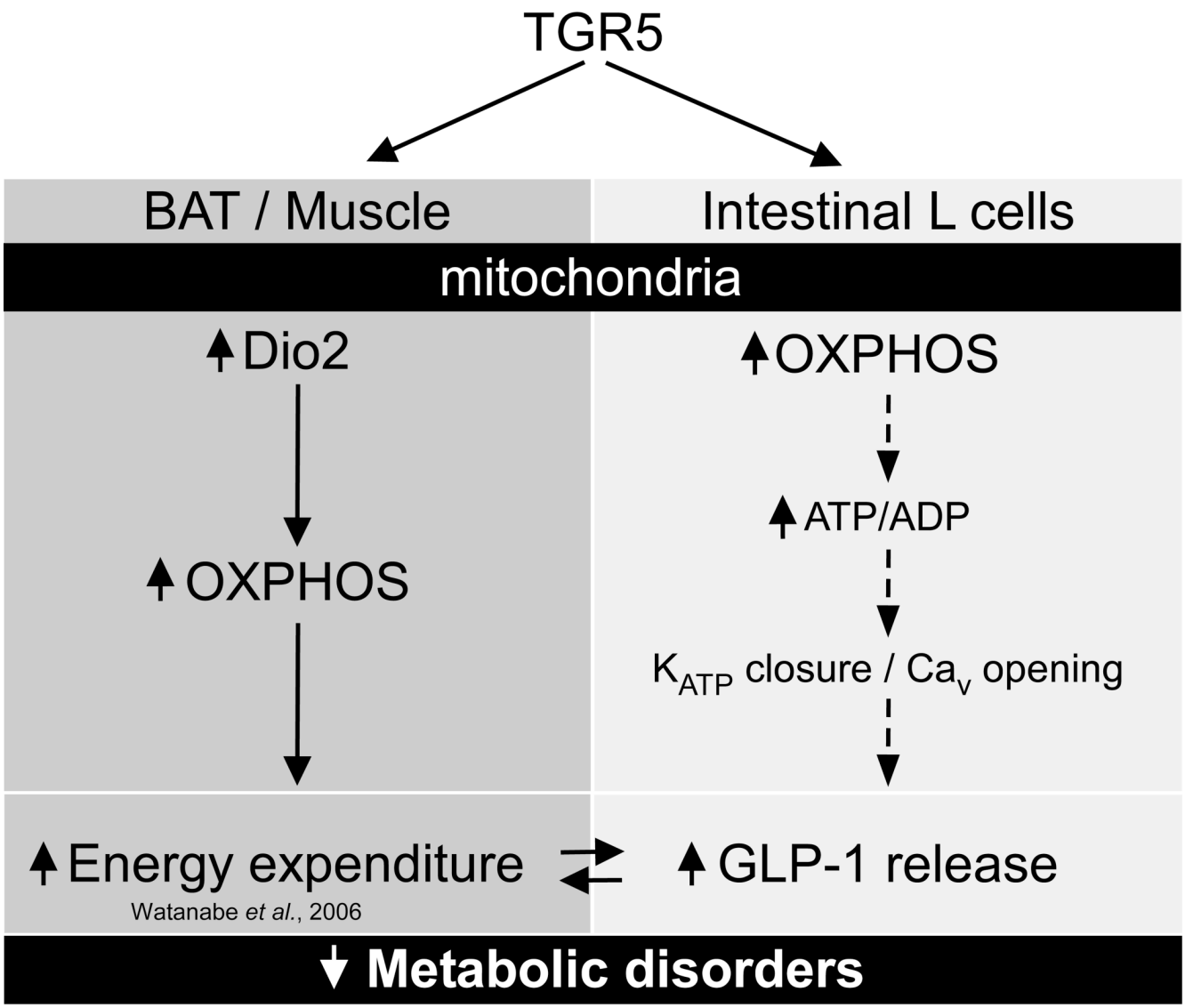

Figure 7. TGR5-mediated bile acid sensing maintains metabolic function

In brown adipose tissue (mouse) and in skeletal muscle (human), TGR5 activation triggers an increase in mitochondrial oxidative phosphorylation (OXPHOS) which results in energy expenditure and helps prevent obesity in mice treated with TGR5 agonists. Here, we demonstrated that in enteroendocrine L-cells, TGR5 activation also triggers an increase in mitochondrial OXPHOS, which is associated to a rise in the ATP/ADP ratio and a subsequent closure of the ATP-dependent potassium channel (K_{ATP}) and calcium mobilization (Ca_v). As a consequence, release of the incretin glucagon-like peptide-1 (GLP-1) is increased which helps explain the improvement of glucose homeostasis in obese mice treated with a TGR5 agonist.